ARCHIVES OF ELECTRICAL ENGINEERING VOL. 69(2), pp. 287–302 (2020)

DOI 10.24425/aee.2020.133026

A coefficient diagram method based AGC mechanism for an interconnected power system in coordination with UPFC and AC/DC link

A.K. Sahani, Ravi Shankar, Murali Sariki, Rajib Kumar Mandal

National Intitute of Techonology Patna
Bihar, India
e-mail: ravi@nitp.ac.in

(Received: 12.07.2019, revised: 08.01.2020)

Abstract: Frequency regulation is in a first line of preference for an interconnected power system. Presence of nonlinearities in the generation systems further raises the complexity level of the problem. In this scenario, this article presents a robust Automatic Generation Control (AGC) mechanism to maintain the frequency and tie-line power of the power system to their nominal values. A Coefficient Diagram Method (CDM) based AGC mechanism including an AC/DC tie-line and Unified Power Flow Controller (UPFC) has been developed and the performance in handling the frequency regulation has been analyzed. The nonlinearities such as Governor Dead-Band (GDB) and Generation Rate Constraint (GRC) are included in the system to analyze the proposed AGC scheme in a more realistic approach. The AC/DC tie-line and UPFC which are included in the proposed AGC scheme provides an immense strength to handle the active power variation as-well-as frequency regulation. To develop a more effective AGC scheme, the parameters of an AC/DC tie-line and UPFC are optimized by successful implementation of the Fruit Fly Optimization Algorithm (FOA). The justification of the proposed AGC scheme has been carried out through a step by step verification such as justifying the CDM based controller, effectiveness of the proposed scheme and robustness of the system against parameters variation. The CDM based controller has been compared with the conventional controllers to elevate the effectiveness and the supremacy of the proposed AGC scheme has been examined by comparing with previously published work. The design and simulation of the work has been carried out by the MATLAB/Simulink® tool box.

Key words: AGC, AC/DC link, CDM, GDB, GRC, UPFC

1. Introduction

In this contemporary world, the size and complexity of the power system have been increasing at a swift pace. In this scenario, supplying quality power to the costumers is an important task present in front of the electricity suppliers. Among the different power quality issues, frequency regulation is concentrated in this article. Dynamics in load demand causes the deviation in frequency and tie-line power from nominal values. AGC mechanism is a preferable solution for this problem, which poses two control levels named as primary and secondary frequency regulation. An effective controller at secondary frequency regulation level improves the dynamic response. There are several fixed parameter controllers such as conventional controllers, cascaded topologies and 2-degree freedom-controllers for the secondary frequency regulation level are detailed in [3–5]. Operating conditions of the modern power system may vary from time to time and hence, it is important to develop an efficient controller which is suitable to all operating conditions. Previous studies investigated fuzzy logic, artificial neural network and genetic algorithm based controllers for suitability to different operating conditions and to mitigate backdrops of the conventional controllers [6–8]. Despite desired results, the complication in algorithms and displeased transient response encouraged the researchers to focus on some other elegant approach to the AGC mechanism. As part of the progress, a Coefficient Diagram Method (CDM) to handle the frequency and tie-line power variations is proposed in [9] for an interconnected power system. On the other hand, the researcher's provided effective alternatives to handle the active power variation. Articles [10–14] presented the accomplishment of improved dynamic response by using energy storage systems and Flexible AC Transmission System (FACTS) devices. Several FACTS devices, such as the Interline Power Flow Controller (IPFC), phase shifters, TCPS, and UPFC etc. have shown an immense effect on the AGC mechanism to acquire better dynamic response [15–18]. Further, the optimistic results obtained by using AC/DC tie-line [19–23] created a strong motivation to develop a CDM based AGC mechanism in coordination with an UPFC and AC/DC tie-line. In the articles mentioned so far, the parameters of the AC/DC tie-line model and UPFC model are fixed. In advance, the FOA technique has been deployed to optimize those parameters within the specified range. The contribution of this article for the research area of the frequency regulation is as detailed below.

The formulation of the CDM based AGC mechanism for single-area as well as two-area interconnected thermal power systems.

- The development of a novel CDM based AGC scheme by inclusion of an UPFC and parallel AC/DC tie-line in the interconnected two area power system.
- The implementation of the fruit fly optimization technique to obtain the parameters of UPFC and parallel AC/DC tie-line models successfully.
- The effectiveness of the proposed AGC scheme has been enhanced by comparing with previously published work.
- The robustness of the proposed scheme has been checked by comparative analysis under the case study of system parameter variations.

The remaining part of this paper has been managed into five more sections. The modeling of the single as well as two area power systems, UPFC and AC/DC tie-line has been discussed in section 2. The development of the CDM based controller is detailed in section 3 and section 4 explores the concept of the fruit fly optimization technique. The discussion of the studies conducted and the conclusion drawn are detailed in remaining sections.

2. Modeling of proposed AGC scheme

The development of an AGC scheme for a two-area interconnected system with inclusion of an AC/DC tie-line and UPFC device has been analyzed with the support of several preliminaries. The parameters of the two-area power system have been taken from the work presented in [9] which is detailed in the appendix.

2.1. Preliminaries

A. Modeling of single-area power system

A single-area power system having a thermal system as generation sources, as depicted in Fig. 1, is considered along with parameters presented in the appendix to develop a basic state space model. The variation in active power demand varies the frequency of the power system. The frequency of the power system can be retained by balancing the generation and load demand. The state space equation of the described power system, having the deviation in frequency (Δf), power outputs of a governor and turbine (ΔP_g and ΔP_{mech}) as state variables and change in load demand (ΔP_L) as well as change in a power command signal (ΔP_0) as input variables, has been derived and expressed in (1)–(3).

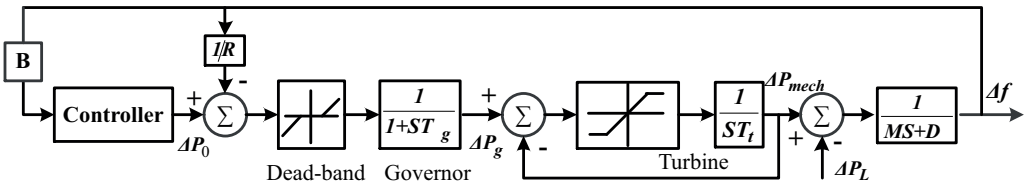

Fig. 1. Block diagram of a single-area thermal power system

$$\Delta \dot{f} = \left(\frac{-D}{M}\right)\Delta f + \left(\frac{-1}{D}\right)\Delta P_L + \left(\frac{1}{D}\right)\Delta P_{\text{mech}}, \tag{1}$$

$$\Delta \dot{P}_g = \left(\frac{1}{T_g}\right)\Delta P_o + \left(\frac{-1}{RT_g}\right)\Delta f + \left(\frac{-1}{T_g}\right)\Delta P_g, \tag{2}$$

$$\Delta \dot{P}_{\text{mech}} = \left(\frac{1}{T_t}\right)\Delta P_g + \left(\frac{-1}{T_t}\right)\Delta P_{\text{mech}}. \tag{3}$$

The state space representation of the single-area power system having deviation in frequency, mechanical power output and governor power output as state variables is given as:

$$\begin{bmatrix} \Delta \dot{f} \\ \Delta \dot{P}_{\text{mech}} \\ \Delta \dot{P}_g \end{bmatrix} = \begin{bmatrix} \frac{-D}{2M} & \frac{1}{D} & 0 \\ 0 & \frac{-1}{T_t} & \frac{1}{T_t} \\ \frac{-1}{R.T_g} & 0 & \frac{-1}{Tg} \end{bmatrix} \begin{bmatrix} \Delta f \\ \Delta P_{\text{mech}} \\ \Delta P_g \end{bmatrix} + \begin{bmatrix} \frac{-1}{D} & 0 \\ 0 & 0 \\ 0 & \frac{1}{T_g} \end{bmatrix} \begin{bmatrix} \Delta P_L \\ \Delta P_o \end{bmatrix}. \tag{4}$$

The area control error is taken as input to the controller which can be given as $\text{ACE} = B\Delta f$.

B. Modeling of UPFC for proposed AGC scheme

Recent developments in power electronics devices encouraged the usage of FACTS devices in the field of power system applications. An UPFC is considered as one of the most flexible and adaptable FACTS devices to handle the stability problems in a tie-line. As mentioned in the introduction section, articles elevated the application of the UPFC in support of an AGC mechanism. The transfer function model of the UPFC, which relates the variation in power supplied against the changes in frequency of the system, has been explained in this section. A schematic diagram of the UPFC for a two-area interconnected power system is as depicted in Fig. 2.

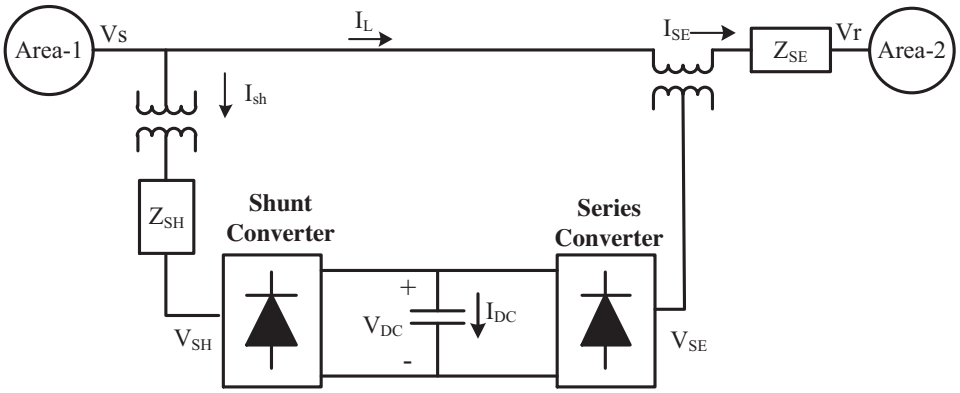

Fig. 2. Connection model of UPFC in a two-area interconnected power system

The complex power at the receiving end of the line can be expressed as:

$$P_{\text{real}} - jQ_{\text{reactive}} = \overline{V_r^*} I_{\text{line}} = \overline{V_r^*} \left\{ \frac{\left(\overline{V_s} + \overline{V_{se}} - \overline{V_r}\right)}{jX} \right\}, \tag{5}$$

where,

$$\overline{V_{se}} = |V_{se}| < (\delta_s - \phi_{se}) \,. \tag{6}$$

Frequency control is possible through the real power control only and hence, from (5) and (6) the expression for real power can be derived as:

$$P_{\text{real}} = \frac{|V_s|\,|V_r|}{X} \sin\delta + \frac{|V_s|\,|V_{se}|}{X} \sin(\delta - \varphi_{se}) = P_o(\delta) + P_{se}(\delta\varphi_{se}), \tag{7}$$

where, V_{se} is the series voltage magnitude of the line and ϕ_{se} is the phase angle of the series voltage. $V_{se} = 0$ depicts the real power of an uncompensated system. The change in the UPFC power injected into the tie-line can be given as:

$$\Delta P_{\text{UPFC}}(s) = \left(\frac{K_{\text{UPFC}}}{1 + sT_{\text{UPFC}}} \right) \Delta F(s). \tag{8}$$

C. Modeling of AC/DC tie-line

The parallel connection of an AC/DC tie-line increases the power transfer capacity with reduced power losses. The transfer function model to enhance the relation between the change in the tie-line power and change in frequency has been described in this section. The power flow from area-1 to area-2 through the AC tie-line can be expressed as:

$$P_{\text{tie,AC}} = P_{12\,\max} \sin(\delta_1 - \delta_2). \tag{9}$$

Subjecting to the linearization of Equation (9), it can be written as:

$$\Delta P_{\text{tie,AC}} = T_{12}(\Delta\delta_1 - \Delta\delta_2), \tag{10}$$

where T_{12} is the synchronizing coefficient of the AC tie-line and it can be given as $T_{12} = P_{12\,\max}\cos(\delta_1 - \delta_2)$. The deviation of the AC tie-line power in terms of frequency can be written as:

$$\Delta P_{\text{tie,AC}} = \frac{2\pi T_{12}}{s}(\Delta F_1 - \Delta F_2). \tag{11}$$

Further, a DC tie-line is considered to be in parallel with the AC tie-line and also assumed that it is working in constant current mode. The change in the DC tie-line power can be expressed as:

$$\Delta P_{\text{tie,DC}} = \left(\frac{K_{\text{DC}}}{1 + sT_{\text{DC}}}\right)(\Delta F_1 - \Delta F_2)\,. \tag{12}$$

Thus the total tie-line power including the effect of the AC/DC tie-line and UPFC is given as:

$$\Delta P_{\text{tie12}} = \Delta P_{\text{tie,AC}} + \Delta P_{\text{tie,DC}} + \Delta P_{\text{UPFC}}. \tag{13}$$

2.2. Modeling of the proposed system

A two-area interconnected power system, each of which having a thermal system as generating sources of the same capacity, has been considered as depicted in Fig. 3. To analyze in a more realistic manner the nonlinearities like a GRC and dead band have been included in each generation system. The modeling of the described system including an AC/DC tie-line and UPFC is as follows below.

The state space equations for the state variables Δf_1, Δf_2, and ΔP_{tie12} can be expressed as:

$$\Delta\dot{f}_1 = \left(\frac{-D_1}{M_1}\right)\Delta f_1 + \left(\frac{-1}{M_1}\right)\Delta P_{\text{AC}} + \left(\frac{1}{M_1}\right)\Delta P_{\text{UPFC}} + \left(\frac{-1}{M_1}\right)\Delta P_{\text{DC}}\,, \tag{14}$$

$$\Delta\dot{f}_2 = \left(\frac{a_{12}}{M_2}\right)\Delta P_{\text{AC}} + \left(\frac{-D_2}{M_2}\right)\Delta f_2 + \left(\frac{a_{12}}{M_2}\right)\Delta P_{\text{UPFC}} + \left(\frac{-1}{M_2}\right)\Delta P_{\text{DC}}\,, \tag{15}$$

$$\Delta\dot{P}_{\text{tie12}} = 2\pi T_{12}\,(\Delta f_1 - \Delta f_2)\,. \tag{16}$$

The state space representation of the described power system having deviation in frequencies and tie-line power as a state variable can be formed from Equations (14)–(16) as:

$$\begin{bmatrix} \Delta\dot{f}_1 \\ \Delta\dot{f}_2 \\ \Delta\dot{P}_{\text{tie12}} \end{bmatrix} = \begin{bmatrix} \dfrac{-D_1}{-M_1} & 0 & \dfrac{-1}{M_1} \\ 0 & \dfrac{-D_2}{-M_2} & \dfrac{a_{12}}{M_2} \\ 2\pi T_{12} & -2\pi T_{12} & 0 \end{bmatrix} \begin{bmatrix} \Delta f_1 \\ \Delta f_2 \\ \Delta P_{\text{tie12}} \end{bmatrix} \begin{bmatrix} \dfrac{1}{M_1} & 0 & \dfrac{-1}{M_1} \\ \dfrac{a_{12}}{M_2} & 0 & \dfrac{-1}{M_2} \\ 0 & 0 & 0 \end{bmatrix} \begin{bmatrix} \Delta P_{\text{UPEC}} \\ \Delta P_{\text{AC}} \\ \Delta P_{\text{DC}} \end{bmatrix}. \tag{17}$$

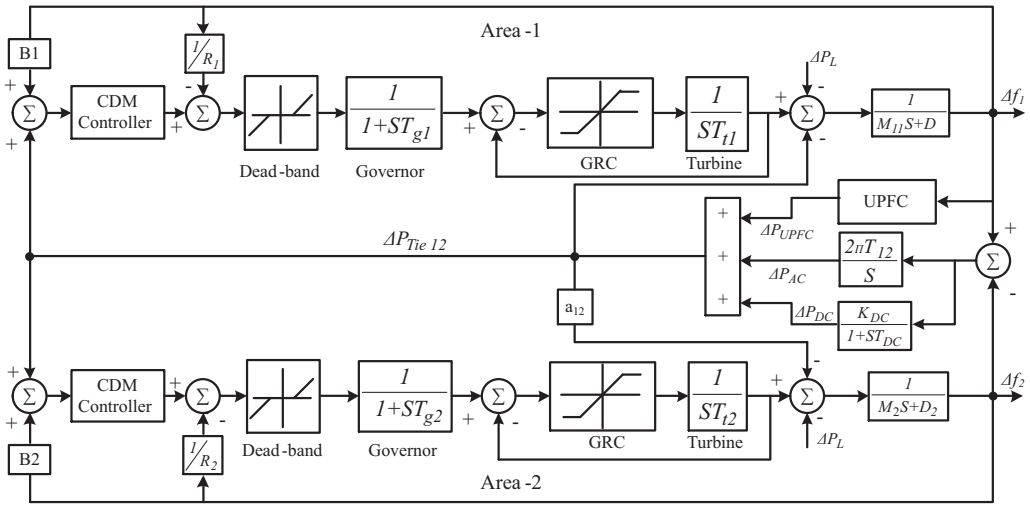

Fig. 3. Block diagram of the proposed two-area inter connected thermal power system

The input to the controller which is ACE can be expressed as summation of biased frequency deviation and deviation in tie-line power. The expressions of the ACE for the considered two-area power system are as given in (18).

$$\mathrm{ACE}_1 = B_1\Delta f_1 + \Delta P_{\mathrm{tie}12}\,, \qquad \mathrm{ACE}_2 = B_2\Delta f_2 + \Delta P_{\mathrm{tie}21}\,. \tag{18}$$

3. Coefficient diagram method (CDM) for AGC mechanism

The CDM belongs to an algebraic type controller design approach, where a Bode plot is replaced by a coefficient diagram. In this method the required response can be acquired by the proper arrangement of the poles of a closed loop transfer function. Providing the stability, robustness, and time response in a single diagram is the beauty of the coefficient diagram. There are two axes present in the coefficient diagram, one is the logarithmic vertical axis and the other is the horizontal axis. The first axis shows the characteristics of the polynomial (a_i), equivalent time constant (τ) and stability indices (γ_i) whereas the next one shows the order (i) values corresponding to each coefficient. The inclination of the curve, degree of convexity and shape of the a_i curve are the measures of the speed of response, stability and robustness of the system, respectively. The designing of CDM controller for this work, carried out by the procedure given in [9].

The block diagram of an LTI system having single-input single-output (SISO) with the CDM controller is depicted in Fig. 4, where $A(S)$, $B(S)$, and $F(S)$ are the forward denominator polynomial, feedback numerator polynomial, and reference numerator polynomial, respectively. The controller has two individual transfer functions and hence the system has two degrees of freedom (2DOF). Further, $R(S)$ is the system reference input, $U(S)$ is the control signal, $D(S)$ is the disturbance signal and $Y(S)$ is the output. Let's assume the transfer function of the plant process

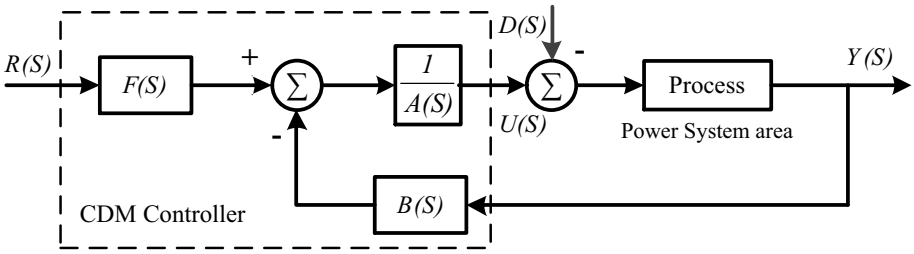

Fig. 4. Block diagram of the CDM controller

is denoted as $N(S)/D(S)$, where $N(S)$ is the numerator polynomial and $D(S)$ the denominator polynomial of the plant transfer function. Thus, the output of the controller is expressed as:

$$Y(S) = \frac{N(S)F(S)}{C(S)}R(S) + \frac{A(S)N(S)}{C(S)}D(S), \tag{19}$$

where $C(S)$ is the characteristic polynomial of the closed-loop system and it can be expressed as:

$$C(S) = A(S)D(S) + B(S)N(S). \tag{20}$$

The control polynomials $A(S)$ and $B(S)$ are defined as:

$$A(S) = \sum_{i=0}^{n} l_i S^i, \qquad B(S) = \sum_{i=0}^{m} k_i S^i (n \geq m). \tag{21}$$

Substituting (21) into (20), we have,

$$C(S) = \sum_{i=0}^{n} l_i S^i D(S) + \sum_{i=0}^{m} k_i S^i N(S) = \sum_{i=0}^{p} a_i S^i, \qquad a_i \geq 0. \tag{22}$$

The relation between the design parameters like τ, γ, stability limit (γ^*) and the coefficients of a characteristic polynomial (a_i) are:

$$\gamma_i = \frac{a_i^2}{a_{(i+1)}a_{(i-1)}}, \qquad i \in [1,\ (n-1)], \quad \gamma_o = \gamma_n = \infty, \quad \tau = \frac{a_1}{a_o}, \tag{23}$$

$$\gamma_i^* = \frac{1}{\gamma_{i-1}} + \frac{1}{\gamma_{i+1}}, \qquad i \in [1,\ (n-1)]. \tag{24}$$

γ_i values are selected as $[2.5, 2, 2, \ldots, 2]$ according to Manabe's standard form, though they can be changed as per the designer's requirement. The target characteristic polynomial with the help of the key parameters can be written as:

$$C_t = a_o \left[\left\{ \sum_{i=2}^{p} \left(\prod_{j=1}^{i-1} \frac{1}{\gamma_{i-j}^{j}} \right) (\tau s)^i \right\} + \tau s + 1 \right], \quad \text{where} \quad C(S) = C_t(S). \tag{25}$$

Finally, the reference polynomial, $F(S)$, can be calculated as:

$$F(S) = \frac{\left(P(S)|_{S=0}\right)}{N(S)}. \tag{26}$$

4. Fruit fly optimization technique

The fruit fly optimization technique is one of the recent optimization techniques in the class of meta-heuristic techniques based on the foraging behavior of the fruit flies. In comparison to other species, a fruit fly has superior sensory perceptions, chiefly its sense of smell and vision. Its range of smell is almost 40km. After detecting the smell of food, a fruit fly, using its sharp vision, finds the food and returns to its companions. This behavior of fruit flies has been described mathematically and utilized to track the global beat solution for several complex problems in the article [24]. By following the same footsteps, the FOA technique is deployed for AGC application in this work. In this current research work, the FOA has been used to optimize the gains (K_{DC}, K_{UPFC}) and time constants (T_{DC}, T_{UPFC}) of an AC/DC link and UPFC, respectively. The optimization of the parameters has been carried out to minimize the objective function given in (27) which is an integral square error (ISE).

$$\mathrm{ISE} = \int_0^t \left(\Delta f_1^2 + \Delta f_2^2 + \Delta P_{\mathrm{tie}}^2\right) \mathrm{d}t. \tag{27}$$

STEPS OF FRUIT FLY OPTIMIZATION ALGORITHM

1	Initialize the number of iterations and the population of a fruit fly swarm.
2	Assign the arbitrary initial location to the fruit fly swarm (i.e for the parameters to be optimised).
3	Assign the direction and distance to each fly randomly, for search of food (to each parameters).
4	Arbitrary set $K_{\mathrm{DC}}(i) = K_{\mathrm{DC}}(1) + \mathrm{random\_value}$ $T_{\mathrm{DC}}(i) = T_{\mathrm{DC}}(1) + \mathrm{random\_value}$ $K_{\mathrm{UPFC}}(i) = K_{\mathrm{UPFC}} + \mathrm{random\_value}$ $T_{\mathrm{UPFC}}(i) = T_{\mathrm{UPFC}} + \mathrm{random\_value}$
5	Evaluate the location of food by smelling, say 'S' (evaluation of fitness of the objective function for different parameters).
6	Identify the fly with maximum smell concentration (minimum value of the objective function work best_obj = min(S)).
7	Assign Lbest = best_obj.
8	Repeat (until the iteration = maximum iteration)
9	Identify the best values obtained for each iteration and its corresponding index
10	Update the global best value.
11	Assign the values obtained to the parameters of an AC/DC tie-line and UPFC.

The optimized values obtained for the parameters of an AC/DC tie-line and UPFC by following the aforementioned steps are $K_{DC1} = 0.05$, $T_{DC1} = 0.1$ s, $K_{DC2} = 0.23$, $T_{DC2} = 0.5$ s, $K_{UPFC} = 0.31$ and $T_{UPFC} = 0.95$ s.

5. Simulation results and analysis

The proposed AGC scheme for the described two-area interconnected power systems has been simulated using the MATLAB/Simulink® toolbox. A CDM controller has been implemented as a secondary level control of an AGC for the thermal system present in the both areas. The effect of the both dead-band and GRC non-linearities are also included to make the system more realistic. The value of the governor dead-band has been taken as 0.05 pu and the GRC is taken to be ±0.00167 pu/s. All the remaining system parameters are taken from [9] and presented in the appendix. The AC/DC tie-line and UPFC are incorporated into the power system tie-line to support the AGC mechanism along with the CDM controller. To get improved dynamic performance, all the gains and time constants of the UPFC and AC/DC tie-line have been optimized using the FOA technique. The proposed scheme of the AGC is investigated step by step, firstly with justification of the controller, secondly comparing with previously published work and lastly robustness check against the parameter variations.

5.1. Justification of the controller

Justification of the controller has been carried out by comparing it with conventional controllers such as an integral (I) controller and proportional-integral (PI) controller on the platform of a single-area power system shown in Fig. 1. A step load of $\Delta P_L = 0.02$ pu at $t = 3$ s has been introduced to study the frequency response of the system. The characteristic polynomial for the system having $\tau = 2$ and the system parameters, given in the appendix, can be expressed as:

$$C_t = 1 + 1.9S + 1.6S^2 + 0.66S^3 + 0.13S^4 + 0.013S^5. \tag{28}$$

The stability indices are $\gamma_{il} = [2.5,\ 2,\ 1.25,\ 5.2]$; $i \in [1,\ 4]$; $\gamma_0 = \gamma_5 = \infty$ and the stability limits are: $\gamma_{il}^* = [0.5,\ 1.2,\ 0.7,\ 0.8]$; $i \in [1,\ 5]$. Taking $k_0 = 1$ and solving Eqs. (19)–(26), the values of control polynomials come out to be:

$$A_i = 0.0075 + 2.8S + 2.4S^2, \qquad B_i = 1 + 1.04S + S^2, \quad \text{where} \quad i \in [1,\ 4]. \tag{29}$$

The dynamic response in terms of frequency deviation, by using conventional controllers and a CDM controller, is as depicted in Fig. 5. It was revealed that an improvement has been accomplished by using the CDM controller in terms of maximum deviation and settling time. The improvement has been in the dynamic response of the system in terms of maximum undershoot and settling time. The obtained values of maximum deviation in frequency and settling time are −0.0487 Hz and 6.75 s, respectively, by using the CDM controller. The numerical details are presented in Table 2. The comparative analysis reveals that there is an improvement of 18.19% and 57.81% accomplished in maximum deviation and settling time, respectively, using the CDM controller compared with the PI controller. The gain values of the I and PI controllers are as tabulated in Table 1, which are obtained by the FOA technique explained in the prior sections.

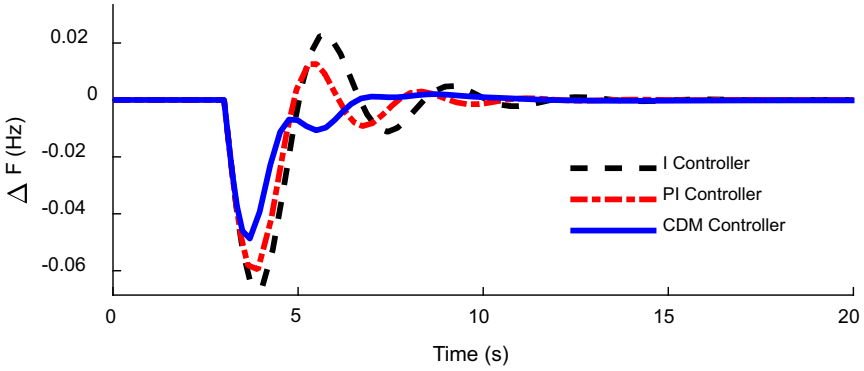

Fig. 5. Comparative analysis of the CDM controller with conventional controller in terms of frequency deviation

Table 1. Gain values of the I and PI controllers

Gains	I controller	PI controller
K_P	–	0.0927
K_I	0.3009	0.3078

Table 2. Comparison of CDM controller with conventional I and PI controllers

	I controller	PI controller	CDM controller	(%) Improvement by CDM controller over PI controller
Maximum deviation in frequency (Hz)	–0.06553	–0.05953	–0.04870	18.19
Settling time (s)	16	12	6.75	57.81

5.2. Supremacy over previously published work

The optimistic results obtained in section 5.1 motivated to develop a CDM based AGC mechanism including an AC/DC tie-line and UPFC. In the process of development of the proposed AGC scheme, the AC/DC tie-line and UPFC are added step by step. The dynamic response of the system for sudden change in load with inclusion of the AC/DC tie-line and UPFC individually is depicted in Fig. 6 and Fig. 7, respectively. Further, the proposed AGC scheme has been examined by comparing with the previous published work [9] under the same platform. A step change in load demand ($\Delta P_{L2} = 0.02$ pu) is applied at $t = 30$ s in area-2 of the described power systems depicted in Fig. 2. For a time constant as $\tau = 2$ s the various parameters of the controller have been calculated as below.

For Area-1

$$C_{t1} = 50 + 100s + 202.36s^2 + 60.9s^3 + 12.51s^4 + s^5 + 0.0098s^6. \tag{30}$$

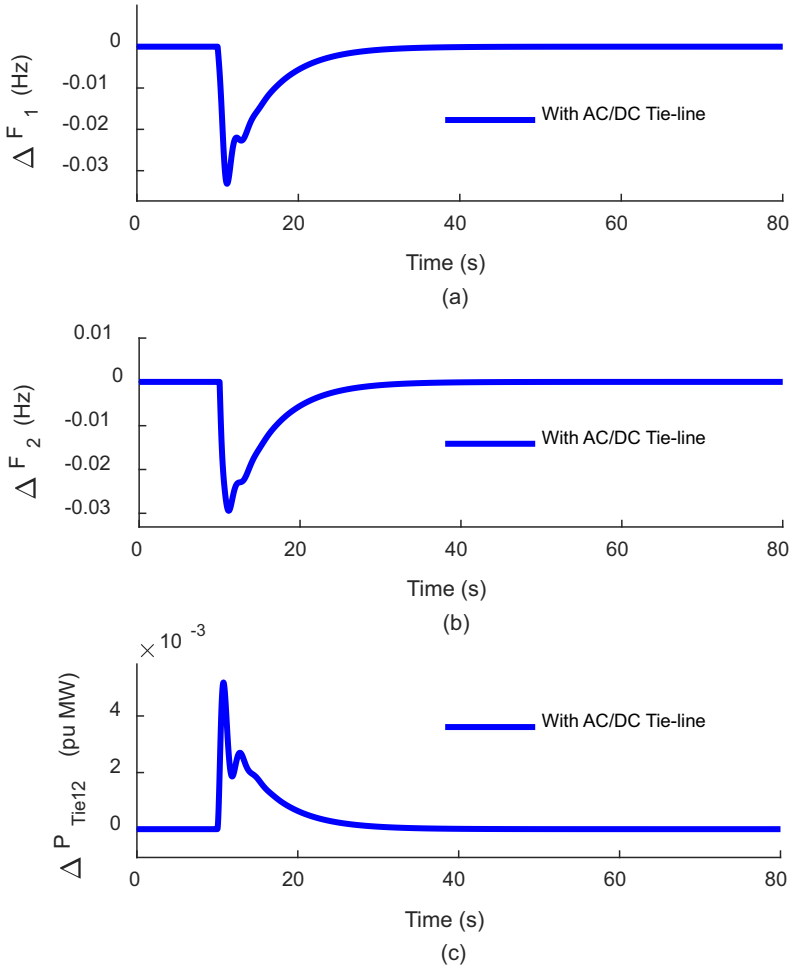

Fig. 6. Dynamic response of the power system including AC/DC tie-line in terms of: (a) frequency deviation of area-1; (b) frequency deviation of area-2; (c) tie-line power deviation

The stability indices are calculated as $\gamma_{i1} = [1,\ 6.5,\ 1.5,\ 2.7,\ 7.2];\ i \in [1,5];\ \gamma_0 = \gamma_6 = \infty$ and the stability limits are $\gamma_{il}^* = [0.15,\ 1.67,\ 0.53,\ 0.67,\ 0.0014];\ i \in [1,\ 5]$. Taking $k_0 = 40$ and solving Eqs. (19)–(26), the values of control polynomials come out to be:

$$A_1 = 148s + 1.98s^2, \qquad B_1 = 40.1 + 69s + 100.01s^2. \tag{31}$$

For Area-2

$$C_{t2} = 39.1 + 80.3s + 161s^2 + 51.3s^3 + 6.5s^4 + 0.606s^5 + 0.0148s^6. \tag{32}$$

The stability indices are calculated as $\gamma_{i2} = [1,\ 6.5,\ 2.2,\ 1.49,\ 3.8];\ i \in [1,\ 5];\ \gamma_0 = \gamma_6 = \infty$ and the stability limits are: $\gamma_{i2}^* = [0.155,\ 1.412,\ 0.826,\ 0.689,\ 0.65];\ i \in [1,\ 5]$. Taking $k_0 = 40$

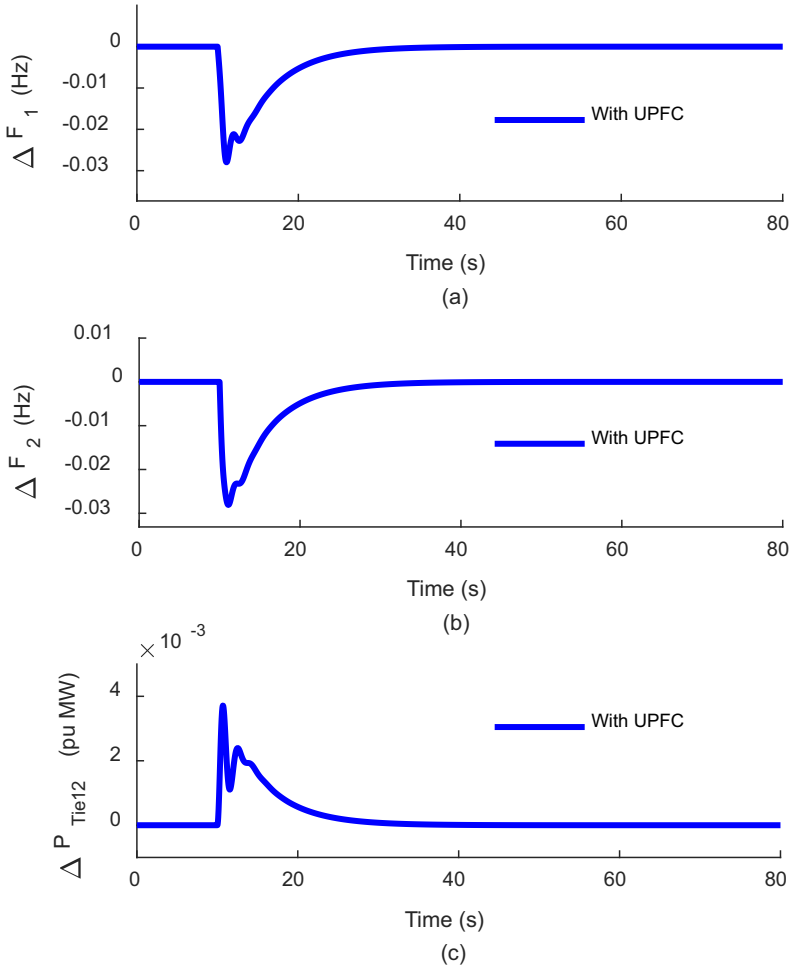

Fig. 7. Dynamic response of the power system including UPFC in terms of: (a) frequency deviation of area-1; (b) frequency deviation of area-2; (c) tie-line power deviation

and solving Eqs. (19)–(26), the values of control polynomials come out to be:

$$A_2 = 57s + 3.04s^2, \qquad B_2 = 32.4 + 52.9s + 100.1s^2. \tag{33}$$

Also, the optimal parameters of the AC/DC tie-line and UPFC, obtained by the FOA optimization are $K_{DC1} = 0.05$, $T_{DC1} = 0.1$ s, $K_{DC2} = 0.23$, $T_{DC2} = 0.5$ s, $K_{UPFC} = 0.31$ and $T_{UPFC} = 0.95$ s. The numerical data analyzed from the dynamic response, depicted in Fig. 8 in terms of maximum deviation in area's frequency and tie-line power, are tabulated in Table 3. The comparative analysis reveals that there is an improvement of 23.88%, 22.35% and 34.23% which has been accomplished over previously published work in terms of maximum deviation in area-1, area-2 frequencies and tie-line power, respectively.

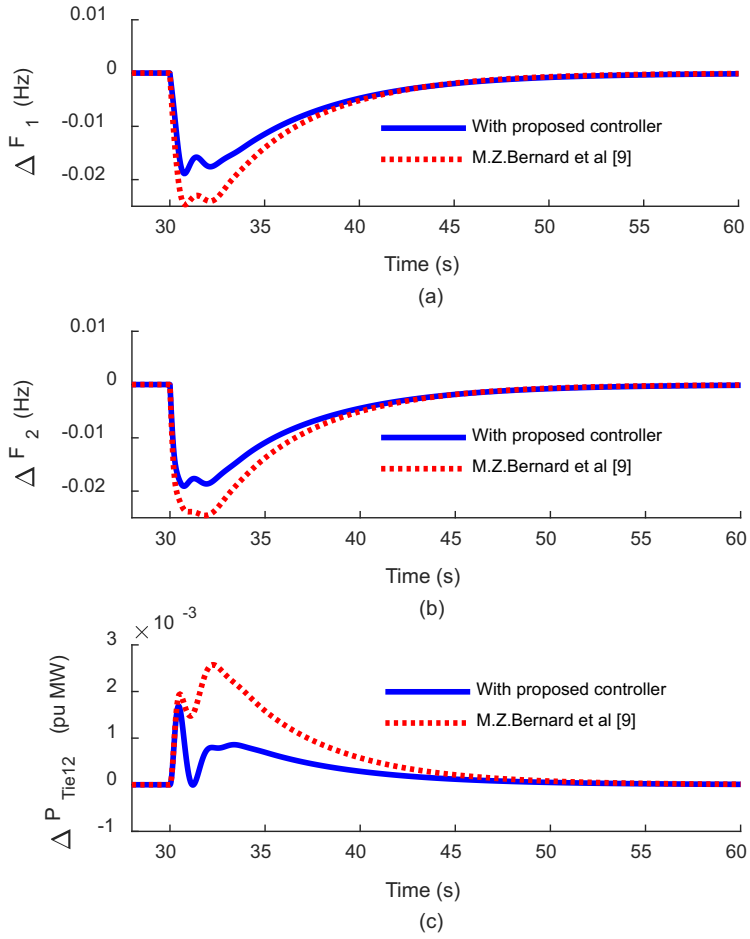

Fig. 8. Comparative analysis with previously published work [9] in terms of: (a) frequency deviation of area-1; (b) frequency deviation of area-2; (c) tie-line power deviation

Table 3. Comparison of proposed AGC scheme with previously published work

Maximum deviation in	**With proposed scheme**	**M.Z. Bernard *et al*. [9]**	**Improvement (%)**
Area-1 frequency (Hz)	−0.0187	−0.0248	24.59
Area-2 frequency (Hz)	−0.0190	−0.0246	22.76
Tie-line power (pu MW)	0.001694	0.002571	34.11

5.3. Robustness analysis

After successful justification of the proposed AGC scheme, it was subjected to robustness verification against variation of system parameters. In this process, the time constants of the governors and turbines in both areas ($T_{g1} = T_{g2} = 0.12$ s, $T_{t1} = 0.052$ s and $T_{t2} = 0.704$ s) and

parameters of rotating mass-load model ($M_1 = 0.2167$ pu.s, $M_2 = 02420$ pu.s, $D_1 = D_2 = 0.02$) have been varied by +25% and −25% of their nominal values. The dynamic response for each case has been verified by using data provided in Table 4. The dynamic response depicted in Fig. 9 reveals the robustness of the proposed AGC scheme against ±25% variation in the system parameters.

Table 4. Robustness analysis of two-area interconnected power system

System parmeter	Nominal	% change in parameters	
		–25%	+ 25%
T_{g1}, T_{g2}	0.12	0.03	0.15
T_{t1}	0.052	0.013	0.065
T_{t2}	0.704	0.176	0.88
M_1	0.2167	0.0541	0.2708
M_2	0.2420	0.0605	0.3025
D_1, D_2	0.02	0.005	0.025

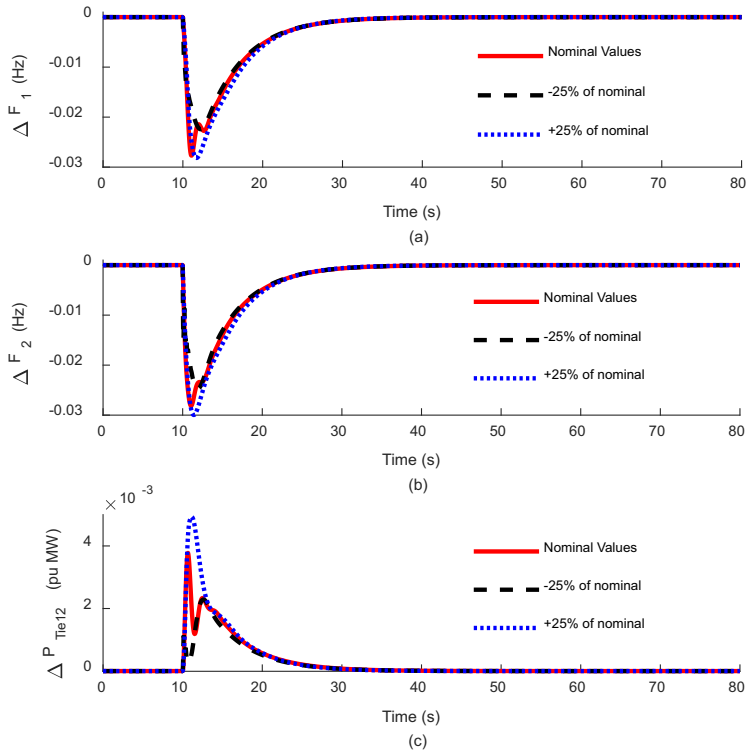

Fig. 9. System dynamic response against the parameter variation: (a) frequency deviation in area-1; (b) frequency deviation in area-2; (c) tie-line power deviation

6. Conclusion

A robust CDM based AGC scheme has been developed for a two-area power system including an AC/DC tie-line and UPFC to maintain the nominal frequency and tie-line power values. In addition, the nonlinearities like a GRC and GDB are included to analyze the power system in a more realistic manner. The assignment of the CDM controller as a secondary level of the AGC, as well as the inclusion of the AC/DC tie-line and UPFC, whose parameters are optimized by the FOA optimization technique, have shown effectiveness by improving the dynamic response of the system. The supremacy of the proposed scheme has been proved by comparing with previously published work and the robustness of the proposed scheme against the parameter variations has been observed. Through the optimistic results observed from this work, it can be concluded that the proposed system is efficient in improving dynamic response against sudden change in load demand.

Appendix

Single area thermal power system: $T_g = 0.08$ s, $T_{t1} = 0.40$ s, $R = 3.0$ Hz/pu, $M = 0.1667$, $D = 0.015$ pu/Hz, $B = 1$.

Two area thermal power system: $T_{g1} = 0.08$ s, $T_{g2} = 0.06$ s, $T_{t1} = 0.40$ s, $T_{t2} = 0.44$ s, $R_1 = 3.0$ Hz/pu, $R_2 = 2.73$ Hz/pu, $M_1 = 0.1667$ pu.s, $M_2 = 0.2017$ pu.s, $D_1 = 0.015$ pu/Hz, $D_2 = 0.016$ pu/Hz, $T_{12} = 0.2$.

References

[1] Kundur P., *Power System Stability and Control*, Electric Power Research Institute, Power System Engineering Series, pp. 1–1199 (1994).

[2] Shankar R., Pradhan S.R., Chatterjee K., Mandal R., *A comprehensive state of the art literature survey on LFC mechanism for power system*, Renew. Sustain. Energy Rev., vol. 76, pp. 1185–1207 (2017), DOI: 10.1016/j.rser.2017.02.064.

[3] Raju M., Chandra Saikia L., Sinha N., *Automatic generation control of a multi-area system using ant lion optimizer algorithm based PID plus second order derivative controller*, Electrical Power and Energy Systems, vol. 80, pp. 52–63 (2016).

[4] Li M., Zhou P., Zhao Z., Zhang J., *Two-degree-of-freedom fractional order-PID controllers design for fractional order processes with dead-time*, ISA Transactions, vol. 61, pp. 147–154 (2016), DOI: 10.1016/j.isatra.2015.12.007.

[5] Saxena S., *Load frequency control strategy via fractional-order controller and reduced-order modeling*, International Journal of Electrical Power and Energy Systems, vol. 104, pp. 603–614 (2019).

[6] Nayak N., Mishra S., Sharma D., Kumar Sahu B., *Application of modified sine cosine algorithm to optimally design PID/fuzzy-PID controllers to deal with AGC issues in deregulated power system*, in IET Generation, Transmission and Distribution, vol. 13, no. 12, pp. 2474–2487 (2019).

[7] Mahdi M.M., Mhawi Thajeel E., Ahmad A.Z., *Load Frequency Control for Hybrid Micro-grid Using MRAC with ANN Under-sudden Load Changes*, 2018 Third Scientific Conference of Electrical Engineering (SCEE), Baghdad, Iraq, pp. 220–225 (2018).

[8] Rerkpreedapong D., Hasanovic A., Feliachi A., *Robust load frequency control using genetic algorithms and linear matrix inequalities*, in IEEE Transactions on Power Systems, vol. 18, no. 2, pp. 855–861 (2003).

[9] Bernard M.Z., Hassan Mohamed T., Soliman Qudaih Y., Mitani Y., *Decentralized load frequency control in an interconnected power system using Coefficient Diagram Method*, Electrical Power and Energy Systems, vol. 63, pp. 165–172 (2014).

[10] Shankar R., Chatterjee K., Bhushan R., *Impact of energy storage system on load frequency control for diverse sources of interconnected power system in deregulated power environment*, Electrical Power and Energy Systems, vol. 79, pp. 11–26 (2016).

[11] Saha A., Saikia L.C., *Combined application of redox flow battery and DC link in restructured AGC system in the presence of WTS and DSTS in distributed generation unit*, IET Gener. Transm. Distrib., vol. 12, no. 9, pp. 2072–2085 (2018).

[12] Tasnin W., Saikia L.C., *Comparative performance of different energy storage devices in AGC of multi-source system including geothermal power plant*, J. Renew. Sustain. Energy, vol. 10, no. 2 (2018).

[13] Dutta A., Prakash S., *Effect of FACTS on load frequency control in deregulated environment*, 7th India International Conference on Power Electronics (IICPE), Patiala, pp. 1–6 (2016).

[14] Lal D.K., Barisal A.K., *Comparative performances evaluation of FACTS devices on AGC with diverse sources of energy generation and SMES*, Cogent Eng., vol. 4, no. 1, pp. 1–29 (2017).

[15] Sekhar Gorripotu T., Kumar Sahu R., Panda S., *AGC of a multi-area power system under deregulated environment using redox flow batteries and interline power flow controller*, Engineering Science and Technology, vol. 18, no. 4, pp. 555–78 (2015).

[16] Bhatt P., Ghoshal S.P., Roy R., *Load frequency stabilization by coordinated control of thyristor controlled phase shifters and superconducting magnetic energy storage for three types of interconnected two-area power systems*, International Journal of Electrical Power and Energy Systems, vol. 32, no. 10, pp. 1111–1124 (2010).

[17] Abraham R.J., Das D., Patra A., *Damping oscillations in Tie-power and area frequencies in a thermal power system with SMES-TCPS combination*, J. Electrical Systems, vol. 7, no. 1, pp. 71–80 (2011).

[18] Chandra Pradhan P., Kumar Sahu R., Panda S., *Firefly algorithm optimized fuzzy PID controller for AGC of multi-area multi-source power systems with UPFC and SMES*, Engineering Science and Technology, an International Journal, vol. 19, no. 1, pp. 338–354 (2016).

[19] Shankar R., Kumar A., Raj U., Chatterjee K., *Fruit fly algorithm-based automatic generation control of multiarea interconnected power system with FACTS and AC/DC links in deregulated power environment*, International Journal of Electrical Power and Energy Systems, vol. 29, no. 1, pp. 1–25 (2019).

[20] Yogendra Arya, Narendra Kumar, Ibraheem Nasiruddin, *AGC of a two-area multi-source power system interconnected via AC/DC parallel links under restructured power environment*, Optim. Control. Appl. Methods, vol. 37, no. 4, pp. 590–607 (2016).

[21] Yogendra Arya, Gupta S.K., Singh N., *Optimal power-frequency control in deregulated thermal, hydro and hydro thermal power systems with AC-DC links*, Recent Advances Elect. Electron. Eng., vol. 12, no. 5, pp. 414–424 (2019).

[22] Yogendra Arya, Narendra Kumar, Gupta S.K., *Load frequency control of a four-area power system using linear quadratic regulator*, International Journal of Electrical Power and Energy Systems, vol. 2, no. 2, pp. 69–76 (2012).

[23] Gupta S.K., Yogendra Arya, Shukla S., Chawala P., *Two-area AGC in interconnected system under the restructured power system using BFO controller*, 6th IEEE power India International Conference, December 5–7, Delhi, India, pp. 1–6 (2014).

[24] Tsao Pan W., *A new Fruit Fly Optimization Algorithm: Taking the financial distress model as an example*, Knowledge-Based System, vol. 26, pp. 69–74 (2012).